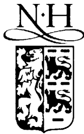

ELSEVIER

Nuclear Instruments and Methods in Physics Research B 178 (2001) 192–195

NIM B
Beam Interactions with Materials & Atoms

www.elsevier.nl/locate/nimb

Structural modifications in amorphous Ge produced by ion implantation

I.D. Desnica-Franković [a,*], K. Furić [a], U.V. Desnica [a], M.C. Ridgway [b], C.J. Glover [b]

[a] Materials Physics Division, R. Boskovic Institute, Bijenicka 54, P.O. Box 1016, 10000 Zagreb, Croatia
[b] Department of Electronic Materials Engineering, Australian Nat. University, Canberra, Australia

Abstract

Raman spectroscopy was used to analyze structural modifications of monocrystalline Ge implanted with 3×10^{12} to 3×10^{16} cm^{-2} ^{74}Ge ions, at either room temperature (RT) or liquid nitrogen (LN) temperature. In all implanted samples, beyond the amorphization threshold dose ($\simeq 10^{14}$ cm^{-2}), a dose-dependent evolution of the amorphous matrix could be followed. However, changes induced in samples implanted at −196°C (LN) differed from those implanted at 21°C. Characteristic Raman parameters relevant for disorder assessment suggest relaxation of the amorphous network with ion dose in samples implanted at RT in contrast to the LN temperature samples, in which additional implantation produces further disordering. These findings are consistent with the results obtained by extended X-ray absorption fine structure spectroscopy (EXAFS) wherein again both a dose- and temperature-dependent evolution of the inter-atomic distance distribution was observed. © 2001 Elsevier Science B.V. All rights reserved.

Keywords: Amorphous Ge; Ion implantation; Disorder; Raman spectroscopy; EXAFS

1. Introduction

Implantation induced disorder is of great interest for both basic understanding and technological applications since ion beam processing is a powerful and versatile tool in many areas of technology. It has been extensively documented that ultimate properties of the processed material strongly depend on the implantation parameters and post-implantation treatments [1–5]. The findings also suggested that different initial microstructure in disordered network led to substantial differences in the 'end-material' [4]. In the present study, we have used Raman spectroscopy and extended X-ray absorption fine structure spectroscopy (EXAFS) to analyze structural modifications of Ge samples which have been implanted by different doses of ^{74}Ge, ranging from very low to very high doses, two orders of magnitude beyond the amorphization dose.

2. Experimental

Monocrystalline Ge samples were implanted with 500 keV ^{74}Ge ions, doses ranging from 3×10^{12}

* Corresponding author. Fax: +385-1-4680-114.
E-mail address: ddesnica@rudjer.irb.hr (I.D. Desnica-Franković).

0168-583X/01/$ - see front matter © 2001 Elsevier Science B.V. All rights reserved.
PII: S0168-583X(00)00489-4

to 3×10^{16} cm^{-2}, at either 21°C (RT) or liquid nitrogen (LN) temperature (−196°C). After the implantation, the samples were initially characterized by Rutherford back-scattering (RBS) and then analyzed by Raman scattering (RS) and EXAFS. First-order RS spectra were obtained using a DILOR Z-24 triple spectrometer and excitation with the 514.5 nm line from an Ar-ion laser [4]. We have analyzed Raman parameters relevant for the disorder assessment. In all computations in this work, we refer to the reduced Raman intensity $I_R(\omega)$ with the thermal Bose–Einstein and harmonic oscillator factors removed so that $I_R(\omega) = I(\omega)\omega/[n(\omega)+1]$, where $I(\omega)$ is the measured intensity. Transmission EXAFS measurements at the Ge K edge were performed at 12 K; data were extracted from the absorption spectra in a conventional manner. Details are given in [6].

3. Results and discussion

Fig. 1 depicts a gamut of reduced Raman spectra for Ge samples. Only the samples implanted at doses beyond the amorphization threshold are presented. Raman bands characteristic for a-Ge could be differentiated: the TO-like mode at ≈270 cm^{-1}, TA at ≈70 cm^{-1}, and contributions of two even broader bands, LA at ≈170 cm^{-1} and LO at ≈245 cm^{-1}. The intense crystalline transversal optical TO(Γ) peak at 300 cm^{-1} is given for a comparison in Fig. 1(a).

The intensity ratio of the TA to TO peak (I_{TA}/I_{TO}) as a function of ion dose has been determined for both implantation temperatures and presented in Fig. 2(a). For doses 3×10^{12} to 3×10^{13} cm^{-2} both types of samples are predominately crystalline and Raman spectra were dominated by the crystalline TO peak. The 10^{14} cm^{-2} implanted sample at RT, represents a transition to a completely amorphous material obtained for higher doses. The I_{TA}/I_{TO} intensity ratios describe structural characteristics of the amorphous matrix related to the intermediate range order [7]. The ratio increases with disorder. Hence, the pronounced decrease of the I_{TA}/I_{TO} ratio for doses 3×10^{14} to 3×10^{16} cm^{-2} in RT samples is a clear sign of the network relaxation, assisted with vacancy clustering and porosity induced with doses $\geqslant 10^{16}$ cm^{-2} [6]. On the contrary to RT samples, the I_{TA}/I_{TO} ratio in LN samples stays almost constant throughout the whole range of implanted doses.

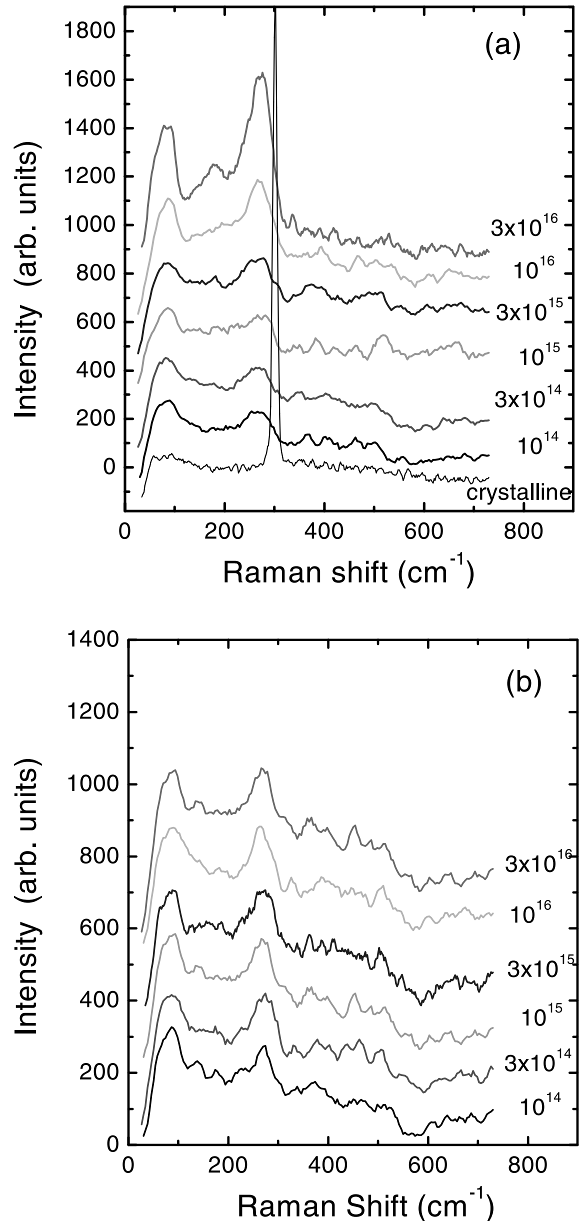

Fig. 1. Room temperature Raman spectra of a-Ge for different ion doses (in cm^{-2}) implanted at (a) 21°C, (b) −196°C.

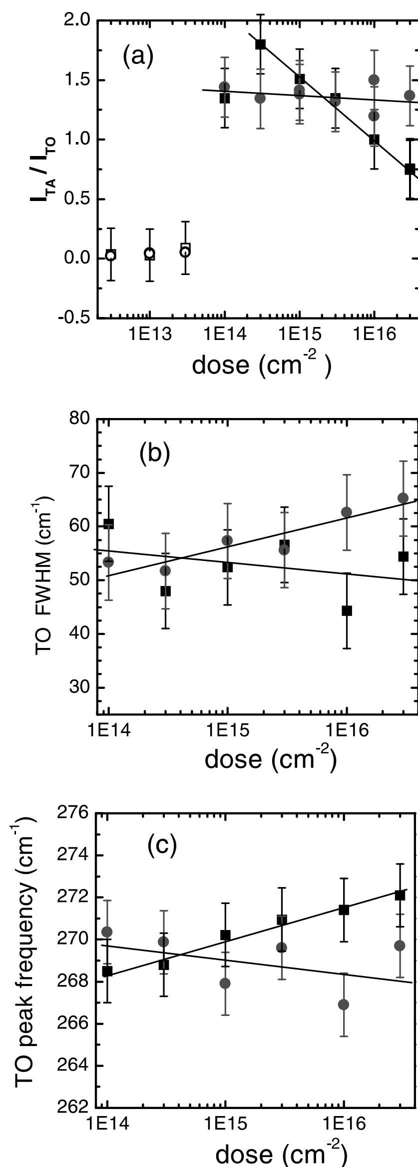

Fig. 2. Ion dose dependence of (a) TA to TO intensity ratio, (b) band-width, (c) frequency position of the TO-like peak in a-Ge, implanted at (■) RT and (●) LN temperature.

Fig. 2(b) depicts changes in the width of the TO-like peak, Γ_{TO}. In LN samples a progressive increase from $\Gamma_{TO} \approx 52$ cm^{-1} to $\Gamma_{TO} \approx 64$ cm^{-1} as a function of ion dose was measured, suggesting increased disorder within the amorphous network. According to [8] the Γ_{TO} increase in LN samples would correspond to an increase in bond angle distribution width, $\Delta\theta$, for $\sim$2.4°, accompanied by an increase of strain energy stored in distorted tetrahedral bonds [9]. In RT implanted samples, a reduction in the TO-like band-width of $\sim$10%, indicates a decrease of bond strain, leading to structural relaxation of the a-Ge matrix.

The TO peak location frequency, ω_{TO}, is presented in Fig. 2(c). The ω_{TO} in RT samples shifts progressively to higher frequencies, toward the position of the crystalline TO, whereas in LN sample it moves even further away. The frequency of phonon bands is a function of inter-atomic forces; specifically, in amorphous materials a decrease in ω_{TO} is associated with an increased number of dangling bonds. The results in Fig. 2(c) imply that a notable defect diffusion has occurred in RT samples during implantation, since dangling bonds (or vacancy–interstitial pairs) can only anneal via bimolecular recombination [10].

Figs. 3(a) and (b) show ion dose and implant-temperature dependence of the structural parameters of a-Ge, as obtained by EXAFS. For LN samples the bond length C^*_{1s} progressively increased as a function of dose with a significantly lesser change apparent for RT samples. Furthermore, an increase in asymmetric deviations of the inter-atomic distance distribution from Gaussian behavior as a function of dose was observed for LN samples, whereas, again, a lesser change was apparent for RT samples (Fig. 3(b)). The first shell coordination number was ion dose independent for both implant temperatures, not differing from the crystalline reference. This is concordant with general retention of tetrahedral coordination in the local atomic environment. EXAFS results suggest that in −196°C-implanted samples structural modifications resulted from an increase in the three- and five-fold coordinated atom fractions and represent a mechanism of accommodating vacancy- and interstitial-like defects within the amorphous phase. The lesser change in structural parameters for 21°C-implanted samples are consistent with the reduced fraction of point defects due to increased defect mobility and dynamic annealing [6]. The difference between EXAFS and RS results on RT samples could be due to the differences in two techniques – EXAFS and RS being sensitive to bond length and

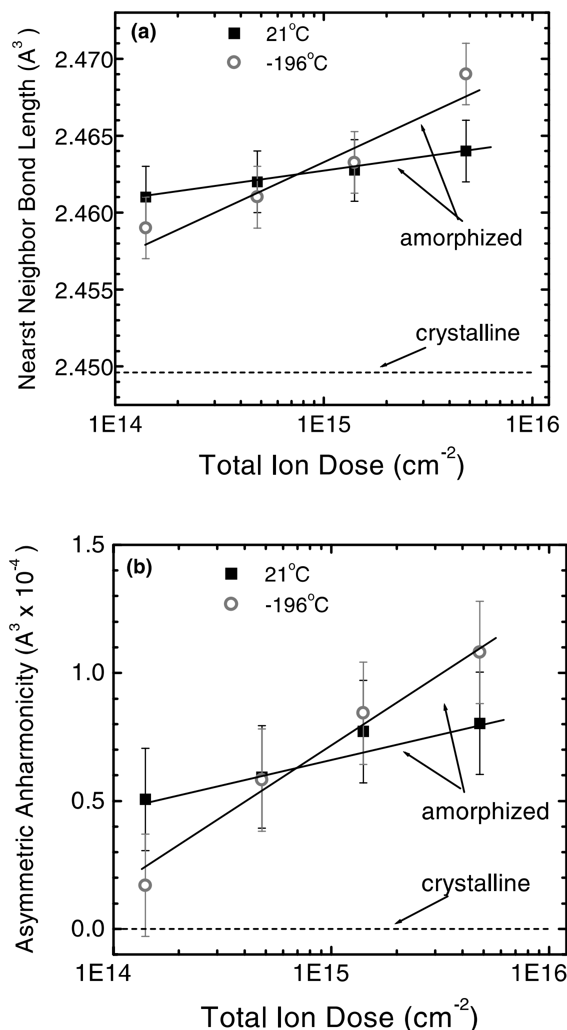

Fig. 3. Nearest-neighbor bond length C^*_{1s} and (b) asymmetric anharmonicity C^*_{3s} as a functions of ion dose and implant temperature.

bond angle changes, respectively. Hence, we can speculate that the equilibrium structure at RT involves bond length distortion but bond angle relaxation.

4. Conclusions

In conclusion, we have demonstrated by Raman scattering and EXAFS spectroscopy that the microstructure in amorphous Ge continuously evolves as a function of ion dose, but the changes differ depending on implant temperature. In samples implanted at 21°C, as evidenced by RS, thermal energy, in addition to the energy supplied by implantation, has been sufficient to induce transformations to the lower free energy configurations within the amorphous matrix. RT enabled diffusion and restructuring of defects, including the onset of porosity, resulting in lesser strain in distorted bonds, thus leading to an overall more relaxed network. However, EXAFS indicated minor increase in disorder at RT as well. All the relaxation processes were impeded in samples implanted at −196°C, in which an ion dose-dependent increase in defective configurations, including both increased number of defects and short-range disorder, was observed by both techniques.

Acknowledgements

The research has been supported by the Ministry of science and Technology of the Republic of Croatia. M.C.R. and C.J.G. were supported by the Australia Synchrotron Research Program, funded by the Commonwealth of Australia.

References

[1] T.E. Haynes, O.W. Holland, Appl. Phys. Lett. 58 (1991) 452.
[2] T.E. Haynes, O.W. Holland, Appl. Phys. Lett. 59 (1991) 452.
[3] S. Roorda, W.C. Sinke, J.M. Poate, D.C. Jacobson, S. Dierker, B.S. Dennis, D.J. Eaglesham, F. Spaepen, P. Fuoss, Phys. Rev. B 44 (1991) 3702.
[4] I.D. Desnica-Frankovic, J. Appl. Phys. 85 (1999) 7587 and references therein.
[5] U.V. Desnica, I.D. Desnica-Franković, M. Ivanda, K. Furić, T.E. Haynes, Phys. Rev. B 55 (1997) 16205 and references therein.
[6] M.C. Ridgway, C.J. Glover, K.M. Yu, G.J. Foran, C. Clerc, J.L. Hansen, A. Nylandsted Larsen, Phys. Rev. B 61 (19) (2000) and references therein.
[7] G. Morell, R.S. Katiyar, S.Z. Weisz, H. Jia, J. Shinar, I. Balberg, J. Appl. Phys. 78 (1995) 5120.
[8] R. Tsu, J. Gonzalez-Hernandez, P.H. Pollak, Solid State Commun. 54 (1985) 447.
[9] W.C. Sinke, S. Roorda, J. Mater. Res. 3 (1988) 1201.
[10] P.A. Stolk, F.W. Saris, A.J.M. Berntsen, W.F. van der Weg, L.T. Sealy, R.C. Barklie, G. Kroetz, G. Mueller, J. Appl. Phys. 75 (1994) 7266.